International Journal on Recent and Innovation Trends in Computing and Communication
ISSN: 2321-8169 Volume: 11 Issue: 10
Article Received: *20 August 2023* ***Revised:*** *10 October 2023* ***Accepted:*** *24 October 2023*

Whale Optimization Algorithm with Fuzzy Wavelet Neural Network for Pneumonia Detection and Classification

[1,*]Parthasarathy V., [2]Saravanan S.
[1]Department of Computer Science,
Dr. M.G.R. Government Arts and Science College for Women,
Villiupuram, Tamilnadu.
sarathympt@gmail.com
[2]Department of Computer and Information Science,
Annamalai University, Annamalai Nagar,
Chidambaram, Tamilnadu.
aucissaran@gmail.com

Abstract—Pneumonia detection and classification are a vital medical imaging task that purposes to automatically recognize and classify pneumonia-related abnormalities in chest radiographs or Chest X-Ray (CXR) imaging. Accurate and prior identification of pneumonia is important for suitable treatment and recovering patient results. The main drive is to recognize whether an X-ray image indicates the presence of pneumonia or not. A binary classification techniuqe is trained to distinguish normal and pneumonia X-rays. Deep Learning (DL) approaches are revealed major success in automating this process, assisting healthcare specialists in analyzing pneumonia more effectively. This article presents a Whale Optimization Algorithm with Fuzzy Wavelet Neural Network for Pneumonia Detection and Classification (WOAFWNN-PDC) technique on CXRs. The purpose of the WOAFWNN-PDC technique is to apply optimal DL approaches for the recognition and classification of pneumonia. In the presented WOAFWNN-PDC technique, Gaussian Filtering (GF) approach is used for the noise removal process. In addition, the MobileNetv3 model is utilized for the feature extraction method. Moreover, the FWNN technique was applied to the classification of pneumonia. Finally, the WOA can be executed for an optimum selection of the parameters related to the FWNN approach. The simulation value of the WOAFWNN-PDC algorithm was assessed on a benchmark medical database. The comparative analysis exhibits better results than the WOAFWNN-PDC technique.

Keywords- Medical imaging; Pneumonia; Computer vision; Whale optimization algorithm; Deep learning.

I. INTRODUCTION

Pneumonia is a lung contamination, which usually appears in both lungs and either the right or left lungs simultaneously, impacting the alveoli which are tiny air sacs in the lungs [1]. The many signs of pneumonia such as chest pain, shortness of breath, fever, and dry cough. As stated by the World Health Organisation (WHO), the greatest method to diagnose pneumonia is recently Computed Tomography (CT) [2]. Additionally, imaging is an essential part of detecting and managing pneumonia, developed to be image analysis must always start with traditional radiography, and CT can be only needed when the radiography outcomes are undetermined. A CXR is highly frequently suggested to patients with undefined reasons for pneumonia [3]. Chest films or radiographs employ ionizing radiation as X-rays which are like any other techniques of radiography [4]. The chest film produces chest images. Since a CXR, pneumonia has been categorized into four types namely interstitial pneumonia, lobular pneumonia, lobar pneumonia, and bronchopneumonia [5]. These four various types have quite many differences among patients, varying with distinct classes of pneumonia. Thus, the types of pneumonia can be regarded as challenging tasks. Further, X-ray detections cannot essentially exist in the initial phases of the disease, causing delayed diagnoses; CXR is complex for analysis [6].

The DL technique has a significant Artificial Intelligence (AI) device, which performs a major part in solving several difficult Computer Vision (CV) issues [7]. The DL approaches especially Convolutional Neural Networks (CNNs) are employed expansively for numerous image categorization difficulties [8]. But these methods carry out optimal only while these can be delivered with a huge quantity of information. For biomedical image classification issues, this large quantity of labelled data can be hard for obtaining since it needs that skilled physician categorizes every image, which is a high-cost and time-taking task [9]. Transfer Learning (TL) takes a workaround to surmount this problem. This method is to resolve an issue that includes a smaller database, a method provided training on a huge database is utilized again and network weightage defined in this technique can be implemented [10].

International Journal on Recent and Innovation Trends in Computing and Communication
ISSN: 2321-8169 Volume: 11 Issue: 10
Article Received: *20 August 2023* ***Revised:*** *10 October 2023* ***Accepted:*** *24 October 2023*

This article presents a Whale Optimization Algorithm with Fuzzy Wavelet Neural Network for Pneumonia Detection and Classification (WOAFWNN-PDC) technique on CXRs. The purpose of the WOAFWNN-PDC technique is to apply optimal DL approaches for the recognition and classification of pneumonia. In the presented WOAFWNN-PDC technique, Gaussian Filtering (GF) approach is used for the noise removal process. In addition, the MobileNetv3 model is utilized for the feature extraction method. Moreover, the FWNN approach has been applied to the classification of pneumonia. Finally, the WOA was executed for the optimum selection of the parameters related to the FWNN approach. The simulation value of the WOAFWNN-PDC approach is assessed on a target medical database.

II. RELATED WORKS

Akgundogdu [11] employed ML approaches for estimating the X-ray images. The diagnoses of paediatric pneumonia can be categorized with the developed ML technique by utilizing the CXR images. The suggested technique initially uses a 2D discrete wavelet transform for extracting features from images. In addition, the RF method is utilized for the classification method. A 10-fold cross-validation algorithm can be exploited for estimating the model. In [12], the authors target to design a method that will assist in the classification of CXR medical images into abnormal (sick) and normal (healthy). To accomplish this, 7 recent ML methods and popular CNN techniques are employed for improving accuracy and effectiveness. According to this study, the authors developed DL for the classification task that can be trained with altered images by multi-stages of preprocessing. Abubeker and Baskar [13] targeted to make an innovative and effectual multi-class ML method for detecting and classifying CXR images on GPU. The authors primarily used a geometric extension by a positional transforming function to the unique database for increasing the sample size and aiding forthcoming TL.

Chandra and Verma [14] introduced a technique for the automatic identification of pneumonia on segmented lungs employing an ML model. This study highlights pixels in lungs segmented ROI, which further contribute toward pneumonia diagnosis than the adjacent areas, therefore the features of lungs segmented ROI limited region has been extracted. Hasoon et al. [15] recommended an approach for detecting and classifying COVID19 by image processing through X-ray imageries. A group of processes like preprocessing, segmenting and detecting ROI, feature extracting, and various ML techniques have been implemented.

Shaheed et al. [16] develop a scheme for the automatic identification of pneumonia and COVID19. Primarily, a preprocessing technique depends on Gaussian filtering and a logarithmic operator has been employed to input CXR images. Secondarily, robust features are extracted from CXR images utilizing CNNs and GLCM approaches. Lastly, an RF-ML classifier is employed for classifying images as COVID19, pneumonia, or normal. Habib and Rahman [17] recommended a Gene-based screening algorithm for diagnosing and differentiating corona diseases from pneumonia. This technique employs disease genes for making functional semantic resemblances between genes.

III. THE PROPOSED MODEL

In the present article, an advanced WOAFWNN-PDC method is introduced for classifying and detecting Pneumonia on CXRs. The purpose of the WOAFWNN-PDC technique is to apply optimal DL approach for the recognition and classification of pneumonia. In the presented WOAFWNN-PDC method, several phases of operations are comprised namely GF-based preprocessing, MobileNetv3 feature extractor, WOA and FWNN based tuning and classification. Fig. 1 depicts the entire flow of the WOAFWNN-PDC methodology.

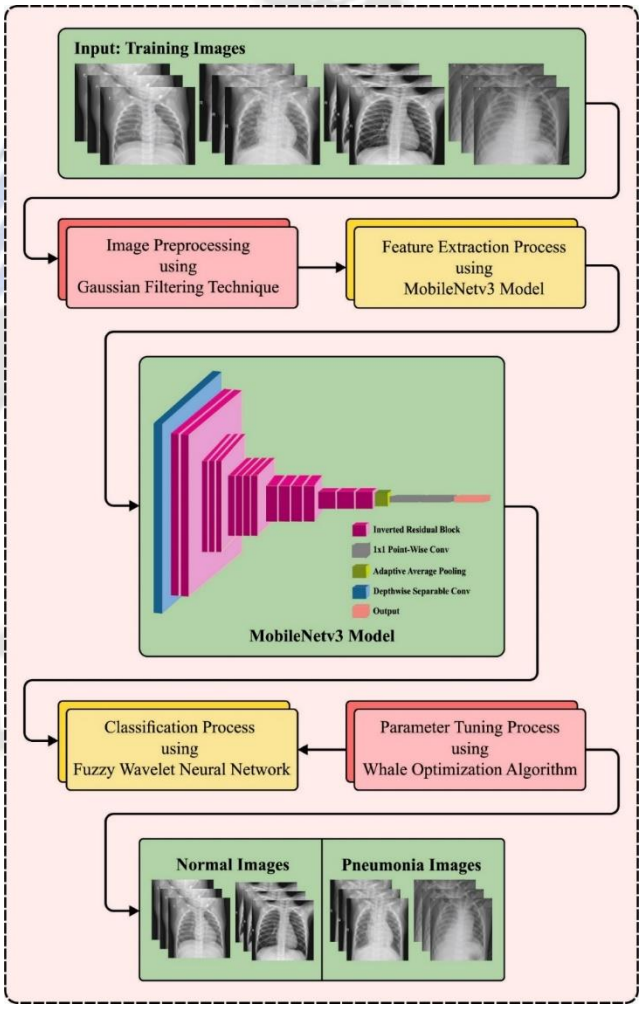

Figure 1. 1 Overall flow of WOAFWNN-PDC method

International Journal on Recent and Innovation Trends in Computing and Communication
ISSN: 2321-8169 Volume: 11 Issue: 10
Article Received: *20 August 2023* ***Revised:*** *10 October 2023* ***Accepted:*** *24 October 2023*

A. Image Preprocessing

For removing the noise in the CXRs, the GF is used. It is an extensively employed image processing approach deployed for blurring or smoothing an image [18]. It is termed after the Gaussian function which is a mathematical function to procedures a bell-shaped curve. The basic concept behind GF is to carry out a weighted average to pixels of images, but the weighted can be defined by the Gaussian kernel. The Gaussian kernel is a 2-D matrix that is determined by its size and Standard Deviation (SD) (sigma). The kernel size defines the extent of the blur outcome, and the SD parameter controls the spread or "strength" of the blur. Higher SD values outcome in an extensive bell-shaped curve and, therefore, stronger smoothing.

B. Feature Extraction

For deriving feature vectors, the MobileNetv3 approach is applied. Mobilenetv3 attained parameters by NAS search [19]. It takes 2 types such as small and large, appropriate for distinct conditions. It receives the depth-wise distinguishable convolutional of Mobilenet_v1 and residual infrastructure with the sequential bottleneck of Mobilenet_v2. Mobilenetv3 employs the NetAdapt technique for obtaining a better count of convolutional channels and kernels. It establishes the SE channel attention infrastructure dependent upon MobileNet_V2 and adjusts the MobileNet_V2 back-end outcome. The network infrastructure of Mobilenetv3 is separated into 3 parts: The primary part contains 1 convolution layer, feature extraction by 3x3 convolutional; the secondary part takes several convolution layers; because of various parameters and levels, separated as small and large versions, the smaller counts is 13 and larger counts is 15; the tertiary part is to decrease parameters and computation, it develops the Avg Pooling, exchanging the whole relation with dual 1x1 convolution layers, and lastly output the type.

C. Image Classification

For the classification process, the FWNN model is utilized. The proposed FWNN methodology combines Wavelet Neural Network (WNN) approach and Fuzzy Neural Network (FNN) approach for classifying [20]. Fig. 2 depicts the architecture of WNN. The network contains 8 layers as defined.

First Layer: An input feature can provide in the 1st layer of the proposed method.

Picture classifying factor, independent parameter, and time sequences are all combined under the current layer. $X = \{X_j | j = 1, \dots, n\}$ is employed for demonstrating the layer.

Second Layer: This layer includes FNN and WNN for estimate. The wavelet has been measured employing the wavelet portion of layers:

$$\psi_{ij}^{k} = \psi\left(\frac{x_j - b_{ij}^{k}}{a_{ij}^{k}}\right), i = 1, \dots, N, j = 1, \dots, n \quad (1)$$

The count of wavelets is formulated as N but the input feature counts are referred to $as\, n$. Concurrently, the transformation of wavelet refers to the display function and reveals its local aspects from the domain of time-frequency.

$$\psi_{a,b} = |a|^{-\left(\frac{1}{2}\right)}\psi\left(\frac{x-b}{a}\right), a, b \in R, a \neq 0 \quad (2)$$

In which, $\psi(x) \in L^2(R)$ defines the wavelet function

$$C_\psi = \int_0^{+\infty} \frac{|\hat{\psi}(\omega)|}{\omega} d\omega < +\infty \quad (3)$$

Let $\hat{\psi}(\omega)$ be the Fourier transform of $\psi(x)$. For stimulating a multivariable process, multidimensional wavelets are presented. In addition, the fuzzy Membership Function (MF) was assessed from the fuzzy area of this layer.

$$\mu_{kj} = e^{-\left(\left(x_j - c_{kj}\right)/\sigma_{kj}\right)^2} \quad (4)$$

In Eq. (4), c_{kj} denotes the centre and σ_{kj} signifies the SD for k^{th} MF.

Third Layer: The layer's outcome is increased and composed with the combination layer. At present, several WNNs can be executed with the N_k wavelet activation function from the wavelet portion.

$$\Psi_i^k = \prod_{j=1}^{n} \Psi_{ij}^k, k, 1, \dots, M \quad (5)$$

Additionally, every node present in this layer specifies one fuzzy rule. The outcome signal (6) is estimated by employing the AND operator.

$$O_k = \prod_{j=1}^{n} \mu_{kj}, k, 1, \dots, M \quad (6)$$

Fourth Layer: The resultant wavelet modules are estimated at layer 4.

R_k: IF x_1 is A_{k1} ... AND x_n is A_{kn},

Then,

$$Y_k = \sum_{i=1}^{N_k} w_i^k \Psi_i^k + \overline{y}_k \quad (7)$$

Assume $x_1, x_2, \dots, x_n$ as the input features, $Y_1, Y_2, \dots, Y_M$ describe the fourth outcome layer, and A_{kj} indicates the k^{th} fuzzy set with typical membership. The weighted bias and matrices are saved from these hidden states as w_i^k and $\overline{y}_k$.

International Journal on Recent and Innovation Trends in Computing and Communication
ISSN: 2321-8169 Volume: 11 Issue: 10
Article Received: *20 August 2023* ***Revised:*** *10 October 2023* ***Accepted:*** *24 October 2023*

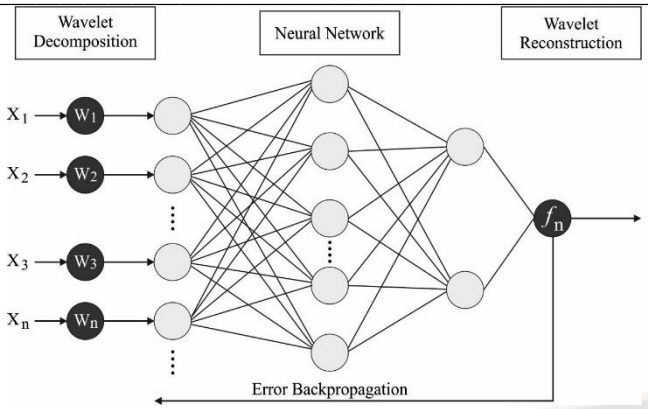

Figure 2. WNN structure

Fifth Layer: The outcome of FNN in O_k and Y_k, the third and fourth layer can be combined with this layer. Layer5 multiplies the layer3 outcome database using the layer4 outcome database.

Sixth Layer: The 2 neurons perform as sum operators for the outcome signals of layer5 and layer3, correspondingly. The quotient was created employing the resultant neuron of layer7 that defines that all the WNN outcomes are equivalent to the proposed FWNNet's performance.

$$O_k^{(5)} = O_k^{(3)} \cdot O_k^{(4)} = O_k \cdot Y_k$$
$$O_1^{(6)} = \sum_{k=1}^{M} O_k^{(5)} \quad (8)$$
$$O_2^{(6)} = \sum_{k=1}^{M} O_k^{(3)}$$

Seventh Layer: The outcome has been collected from the 7th layer.

$$y = O^{(7)} = \frac{O_1^{(6)}}{O_2^{(6)}} = \frac{\sum_{k=1}^{m} O_k\, Y_k}{\sum_{k=1}^{m} O_k} \quad (9)$$

Eighth Layer: This is the ending layer of networks for classifying the factors. It could be a function of activation that changes the data into the outcome layers. The gradient of the main parameter has been measured in the opposite direction, based on $\Theta = (c_{kj}, \sigma_{kj}, b_{ij}^k, a_{ij}^k, w_i^k, \overline{y}_k)$ as follows.

$$E(\Theta, x, y) = \frac{1}{2}(y - f)^2$$
$$\Theta(t+1) = \Theta(t) + \Delta\Theta$$
$$\Delta\Theta = \left(-\gamma_c \frac{\partial E}{\partial c_{kj}}, -\gamma_\sigma \frac{\partial E}{\partial \sigma_{kj}}, -\gamma_b \frac{\partial E}{\partial b_{ij}^k}, -\gamma_a \frac{\partial E}{\partial a_{ij}^k}, -\gamma_w \frac{\partial E}{\partial w_i^k}, -\gamma \frac{\partial E}{y \partial \overline{y}}\right) \quad (10)$$

D. Hyperparameter Tuning

Finally, the WOA adjusts the hyperparameter values of the FWNN model. The WOA is a metaheuristic approach based on humpback whales which have special hunting behaviours used to swim around their target in a shrinking circle which takes a spiral shape and makes bubble-net [21]. WOA mainly comprises exploitation and exploration phases. The exploration stage includes randomly searching for the prey. The exploitation stage contains producing a spiral bubble net and surrounding the prey.

Initially, the humpback whale encircles the target by using Eq. (11). Update the location of whales (searching agent) based on the better solution (target location) using Eq. (12). Adjust A and C parameter vectors for controlling the searching region from the local region by using Eqs. (13) & (14) correspondingly. Decrease the parameter evaluated by Eq. (15) for producing the spiral motion based on Eq. (13).

$$D = \left|C.\vec{X}^*(t) - \vec{X}(f)\right| \quad (11)$$
$$\vec{X}(f+1) = \vec{X}^*(f) - \vec{A}.D \quad (12)$$
$$\vec{A} = 2\vec{a} \cdot \vec{r} - \vec{a} \quad (13)$$
$$\vec{C} = 2.\vec{r} \quad (14)$$
$$a = 2 - t\frac{2}{MAXIter} \quad (15)$$

The spiral-shaped path was inspired by evaluating the distance between $(X*, X)$, the best search agents. Next, the location of the local search agent based on Eq. (16) was evaluated. The D parameter can be measured by Eq. (17). Assume a probability of 50 % between them by using Eq. (18) to model the spiral-shaped path and shrinking encircling shape,

$$\vec{X}(f+1) = D.e^{bl}.\cos(2\pi l) + \vec{X}^*(f) \quad (16)$$
$$D = \vec{X}^*(f) - \vec{X}(f) \quad (17)$$
$$\vec{X}(t+1) = \begin{cases} shrinkingEncircling\ (Eq.(2))\ if\ (p < 0.5) \\ Spiral - shapedpath\ (Eq.(6))\ if\ (p \geq 0.5) \end{cases} \quad (18)$$

The exploration stage of WOA can be optimized by choosing a random search agent for guiding the search process. The arbitrary vector A comprising values lesser than -1 or>1 is employed for forcing the search agent far from the better-known one.

$$\vec{D} = \left|\vec{C}.\vec{X}_{rand} - \vec{X}\right| \quad (19)$$
$$\vec{X}(t+1) = \vec{X}_{rand} - \vec{A}.\vec{D} \quad (20)$$

Where Γ denotes the existing iteration. $\vec{X}^*$ shows the better solution attained. $\vec{X}$ indicates the location vector. A, C stands for co-efficient vector. The vector A in the exploitation and exploration stages sequentially shrinks from two to $zero$ over iteration. r: is a uniform distribution arbitrary integer within $[0,1]$. $MaxIter$ shows the maximal iteration. D indicates the better solution attained. b shows the constant used to determine the logarithmic spiral shape. 1 differs within $[-1,1]$ randomly. P varies randomly in the interval [0,1]. $\vec{X}_{rand}$ shows the randomly chosen whale from the present population.

The fitness selection is a key feature of the WOA method. The encoded outcome was utilized to develop a better solution for candidate results. Later, the value of accuracy is the major condition deployed for constructing a FF.

$$Fitness = \max(P) \quad (21)$$
$$P = \frac{TP}{TP + FP} \quad (22)$$

International Journal on Recent and Innovation Trends in Computing and Communication
ISSN: 2321-8169 Volume: 11 Issue: 10
Article Received: *20 August 2023* ***Revised:*** *10 October 2023* ***Accepted:*** *24 October 2023*

whereas, FP and TP define the false and true positive values.

IV. EXPERIMENTAL VALIDATION

The pneumonia detection outputs of the WOAFWNN-PDC method can be tested employing a dataset from Kaggle repo5sitory [22]. The database includes 1566 normal samples and 4220 pneumonia instances are specified in Table 1. Fig. 3 depicts the normal and Pneumonia images.

TABLE I. DESCRIPTION OF DATABASE

Class	Training	Testing	Validation	Total
Normal	1093	316	157	1566
Pneumonia	2944	854	422	4220

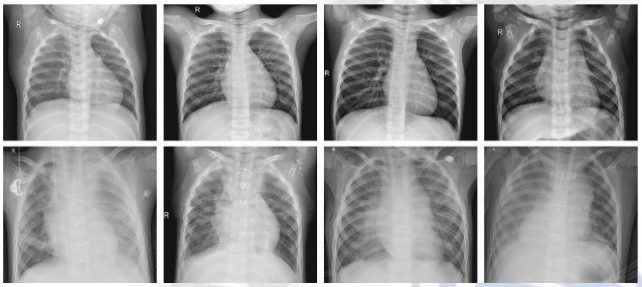

Figure 3. a) Normal b) Pneumonia

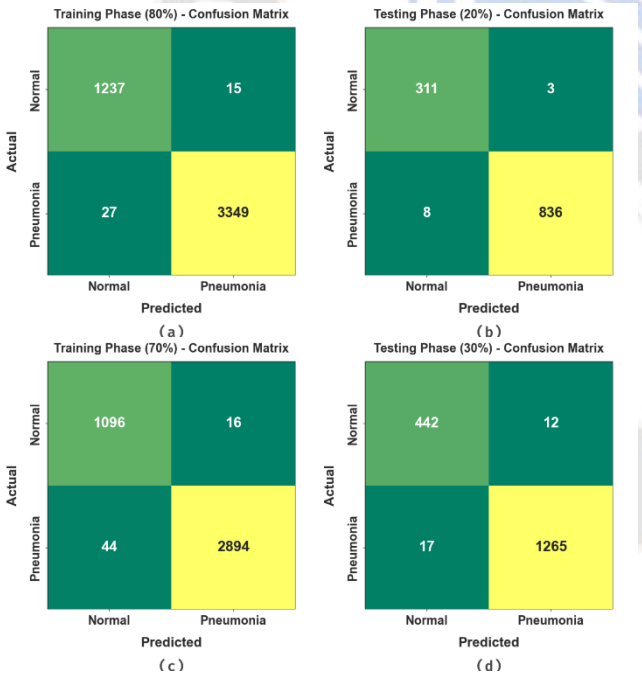

Figure 4. Confusion matrices of (a-b) 80:20 and (c-d) 70:30 of TR/TS set

Fig. 4 exemplifies the confusion matrix presented by the WOAFWNN-PDC methodology at 70:30 and 80:20 of the TR/TS set. The outcome implied that the WOAFWNN-PDC methodology has recognized and classified 2 classes accurately.

TABLE II. PNEUMONIA RECOGNITION OUTPUT OF WOAFWNN-PDC APPROACH ON 80 AND 20 PERCENT OF TR/TS SET

Class	$Accu_y$	$Prec_n$	$Reca_l$	F_{Score}	AUC_{Score}
Training Phase (80%)					
Normal	98.80	97.86	98.80	98.33	99.00
Pneumonia	99.20	99.55	99.20	99.38	99.00
Average	**99.00**	**98.71**	**99.00**	**98.85**	**99.00**
Testing Phase (20%)					
Normal	99.04	97.49	99.04	98.26	99.05
Pneumonia	99.05	99.64	99.05	99.35	99.05
Average	**99.05**	**98.57**	**99.05**	**98.80**	**99.05**

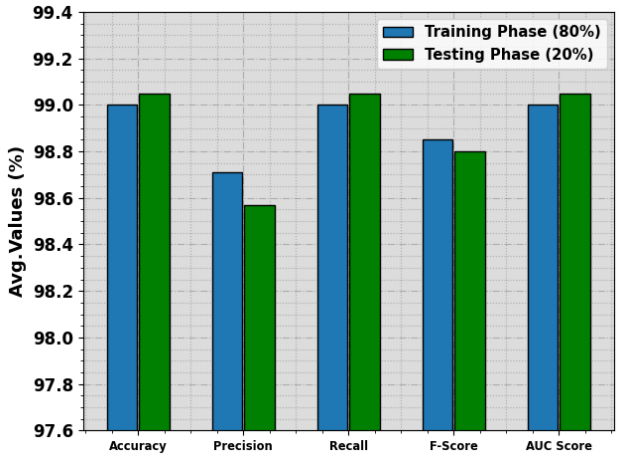

Figure 5. Average output of WOAFWNN-PDC approach on 80 and 20 percent of TR/TS set

The pneumonia recognition outputs under 80:20 of the TR/TS set are stated in Table 2 and Fig. 5. The simulation value shows that the WOAFWNN-PDC methodology properly recognizes two classes. For instance, on 80% of the TR set, the WOAFWNN-PDC methodology attains an average $accu_y$, $prec_n$, $reca_l$, F_{score}, and AUC_{score} of 99.00%, 98.71%, 99.00%, 98.85%, and 99.00% subsequently. Additionally, on 20% of TS set, the WOAFWNN-PDC technique reaches an average $accu_y$, $prec_n$, $reca_l$, F_{score}, and AUC_{score} of 99.05%, 98.57%, 99.05%, 98.80%, and 99.05% correspondingly.

TABLE III. PNEUMONIA RECOGNITION OUTPUT OF WOAFWNN-PDC METHOD ON 70:30 OF TR/TS SET

Class	$Accu_y$	$Prec_n$	$Reca_l$	F_{Score}	AUC_{Score}
Training Phase (70%)					
Normal	98.56	96.14	98.56	97.34	98.53
Pneumonia	98.50	99.45	98.50	98.97	98.53
Average	**98.53**	**97.80**	**98.53**	**98.15**	**98.53**
Testing Phase (30%)					
Normal	97.36	96.30	97.36	96.82	98.02
Pneumonia	98.67	99.06	98.67	98.87	98.02
Average	**98.02**	**97.68**	**98.02**	**97.85**	**98.02**

International Journal on Recent and Innovation Trends in Computing and Communication
ISSN: 2321-8169 Volume: 11 Issue: 10
Article Received: *20 August 2023* ***Revised:*** *10 October 2023* ***Accepted:*** *24 October 2023*

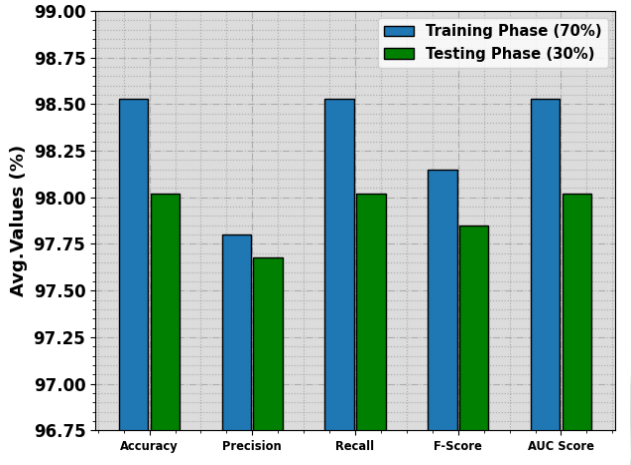

Figure 6. Average output of WOAFWNN-PDC method on 70:30 of TR/TS set

The pneumonia recognition outcomes under 70:30 of the TR/TS set are stated in Table 3 and Fig. 6. The simulation value depicted that the WOAFWNN-PDC algorithm properly distinguishes two classes. For instance, on 70% of TR set, the WOAFWNN-PDC system obtains an average $accu_y$, $prec_n$, $reca_l$, F_{score}, and AUC_{score} of 98.53%, 97.80%, 98.53%, 98.15%, and 98.53% correspondingly. Moreover, on 30% of TS set, the WOAFWNN-PDC algorithm reaches an average $accu_y$, $prec_n$, $reca_l$, F_{score}, and AUC_{score} of 98.02%, 97.68%, 98.02%, 97.85%, and 98.02% correspondingly.

Figure 7. $\boldsymbol{Accu_y}$ curve of WOAFWNN-PDC method on 80 and 20 percent of TR/TS set

Fig. 7 demonstrates the training accuracy TR_accu_y and VL_accu_y of the WOAFWNN-PDC methodology on 80:20 of the TR/TS set. The TL_accu_y is defined by the estimation of the WOAFWNN-PDC methodology on the TR dataset whereas the VL_accu_y is calculated by estimating the performance on a separate testing dataset. The results exhibit that TR_accu_y and VL_accu_y upsurge with an increase in epochs. As a result, the performance of the WOAFWNN-PDC model gets increase on the TR and TS dataset with an increase in the number of epochs.

Figure 8. Loss curve of WOAFWNN-PDC method on 80 and 20 percent of TR/TS set

In Fig. 8, the TR_loss and VR_loss curves of the WOAFWNN-PDC technique on 80:20 of the TR/TS set are shown. The TR_loss defines the error among the predictive outcome and original values on the TR data. The VR_loss represents the measure of the solution of the WOAFWNN-PDC technique on individual validation data. The outcome referred that the TR_loss and VR_loss tend to be lesser with rising epochs. It represented the improved outcome of the WOAFWNN-PDC method and its capability to generate accurate classification. The minimal value of TR_loss and VR_loss determines the improved performance of the WOAFWNN-PDC method in capturing patterns and relationships.

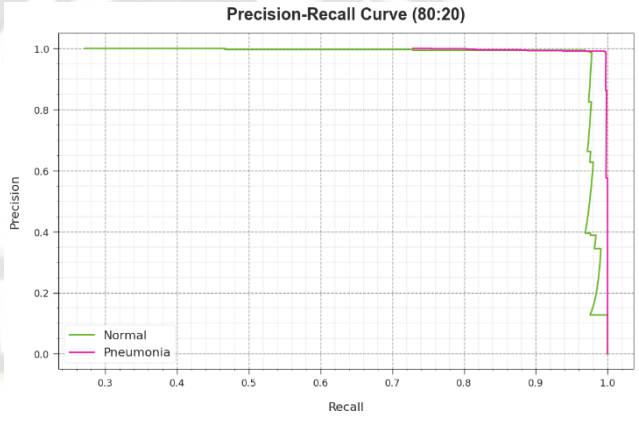

Figure 9. PR curve of WOAFWNN-PDC method on 80 and 20 percent of TR/TS set

International Journal on Recent and Innovation Trends in Computing and Communication
ISSN: 2321-8169 Volume: 11 Issue: 10
Article Received: *20 August 2023* ***Revised:*** *10 October 2023* ***Accepted:*** *24 October 2023*

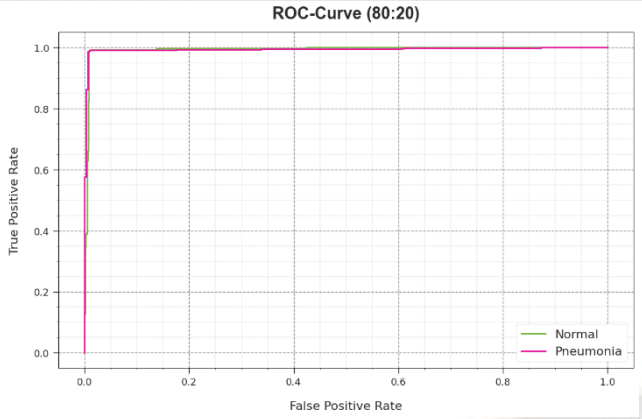

Figure 10. ROC curve of WOAFWNN-PDC method on 80 and 20 percent of TR/TS set

A comprehensive Precision-Recall (PR) analysis of the WOAFWNN-PDC technique is depicted on 80:20 of the TR/TS set in Fig. 9. The simulation values defined that the WOAFWNN-PDC technique outcomes in enhanced values of PR. Moreover, it could be obvious that the WOAFWNN-PDC model obtains improve PR outcomes on 2 classes.

In Fig. 10, a ROC curve of the WOAFWNN-PDC method is exhibited at 80:20 of the TR/TS set. The outputs defined that the WOAFWNN-PDC approach has led to enhanced ROC outcomes. Moreover, it could be stated that the WOAFWNN-PDC approach is achieve improved ROC performances in 2 classes.

Finally, the enhanced performance of the WOAFWNN-PDC technique can be ensured by a comparison study in Table 4 and Fig. 11 [23]. The simulation values stated that the DPC X-Rat-Dl model shows poor performance with the least classification results. At the same time, the visualization-CNN, ADFL-mRMR, and X-ray Images-NN models have obtained certainly boosted results. Along with that, the CNN and CXR-DTL models have shown considerably closer performance. But the promising performance can be accomplished by the WOAFWNN-PDC technique with $accu_y$, $prec_n$, $reca_l$, and AUC_{score} of 99.05%, 98.57%, 99.05%, and 99.05% respectively. These results ensured that the WOAFWNN-PDC technique exhibits promising performance over other models.

TABLE IV. COMPARATIVE OUTPUT OF WOAFWNN-PDC MODEL WITH OTHER METHODOLOGIES

Model	$Accu_y$	$Prec_n$	$Reca_l$	AUC_{Score}
Visualization-CNN	96.20	97.00	98.85	98.56
ADFL-mRMR	96.84	96.88	96.83	96.80
X-ray Images-NN	94.40	94.30	94.50	94.50
DPC X-Rat-Dl	84.50	91.30	89.10	87.00
CNN	98.00	97.00	99.00	98.00
CXR-DTL	98.43	98.26	99.00	99.00
WOAFWNN-PDC	99.05	98.57	99.05	99.05

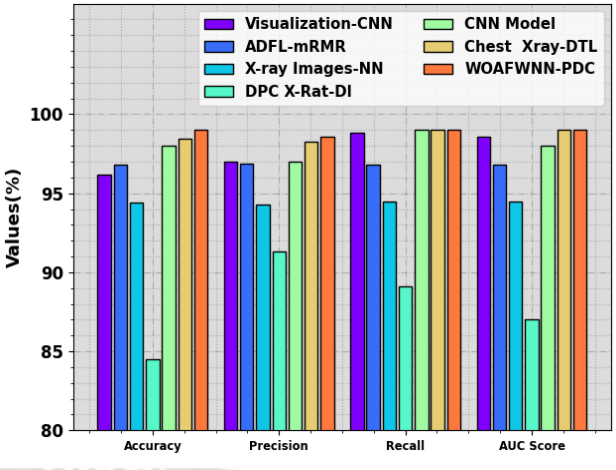

Figure 11. Comparative output of WOAFWNN-PDC model with other approaches

V. CONCLUSION

In this article, a novel WOAFWNN-PDC technique is presented for Pneumonia Detection and Classification on CXRs. The purpose of the WOAFWNN-PDC technique is to apply optimal DL approaches for the recognition and classification of pneumonia. In the presented WOAFWNN-PDC approach, several operation phases are comprised called GF-based preprocessing, MobileNetv3 feature extractor, WOA and FWNN based tuning and classification. In this work, the FWNN approach has been applied to the classification of pneumonia. Finally, the WOA can be executed for the optimum selection of the parameters related to the FWNN approach. The simulation value of the WOAFWNN-PDC approach can be assessed on the targeted medical database. The comparative analysis reveals the better results of the WOAFWNN-PDC approach.

REFERENCES

[1] Kassania, S.H., Kassanib, P.H., Wesolowskic, M.J., Schneidera, K.A. and Detersa, R., 2021. Automatic detection of coronavirus disease (COVID-19) in X-ray and CT images: a machine learning based approach. Biocybernetics and Biomedical Engineering, 41(3), pp.867-879.

[2] Rahman, T., Chowdhury, M.E., Khandakar, A., Islam, K.R., Islam, K.F., Mahbub, Z.B., Kadir, M.A. and Kashem, S., 2020. Transfer learning with deep convolutional neural network (CNN) for pneumonia detection using chest X-ray. Applied Sciences, 10(9), p.3233.

[3] Johri, S., Goyal, M., Jain, S., Baranwal, M., Kumar, V. and Upadhyay, R., 2021. A novel machine learning-based analytical framework for automatic detection of COVID-19 using chest X-ray images. International Journal of Imaging Systems and Technology, 31(3), pp.1105-1119.

[4] Yee, S.L.K. and Raymond, W.J.K., 2020, September. Pneumonia diagnosis using chest X-ray images and machine learning. In proceedings of the 2020 10th international conference on biomedical engineering and technology (pp. 101-105).

[5] Çelik, A. and Demirel, S., 2023. Enhanced Pneumonia Diagnosis Using Chest X-Ray Image Features and Multilayer Perceptron and k-NN Machine Learning Algorithms. Traitement du Signal, 40(3), p.1015.

[6] Katsamenis, I., Protopapadakis, E., Voulodimos, A., Doulamis, A. and Doulamis, N., 2020, November. Transfer learning for COVID-19 pneumonia detection and classification in chest X-ray images. In Proceedings of the 24th Pan-Hellenic Conference on Informatics (pp. 170-174).

[7] Alsharif, R., Al-Issa, Y., Alqudah, A.M., Qasmieh, I.A., Mustafa, W.A. and Alquran, H., 2021. PneumoniaNet: Automated detection and classification of pediatric pneumonia using chest X-ray images and CNN approach. Electronics, 10(23), p.2949.

[8] Chamoli, S. and Tamboli, A.I., 2023. Machine Learning for Early Detection of Pneumonia from Chest X-ray Images. International Journal of Intelligent Systems and Applications in Engineering, 11(7s), pp.111-118.

[9] Kumar, R., Arora, R., Bansal, V., Sahayasheela, V.J., Buckchash, H., Imran, J., Narayanan, N., Pandian, G.N. and Raman, B., 2020. Accurate prediction of COVID-19 using chest X-ray images through deep feature learning model with SMOTE and machine learning classifiers. MedRxiv, pp.2020-04.

[10] Alquran, H., Alsleti, M., Alsharif, R., Qasmieh, I.A., Alqudah, A.M. and Harun, N.H.B., 2021, June. Employing texture features of chest x-ray images and machine learning in covid-19 detection and classification. In Mendel (Vol. 27, No. 1, pp. 9-17).

[11] Akgundogdu, A., 2021. Detection of pneumonia in chest X-ray images by using 2D discrete wavelet feature extraction with random forest. International Journal of Imaging Systems and Technology, 31(1), pp.82-93.

[12] Al Mamlook, R.E., Chen, S. and Bzizi, H.F., 2020, July. Investigation of the performance of machine learning classifiers for pneumonia detection in chest X-ray images. In 2020 IEEE International Conference on Electro Information Technology (EIT) (pp. 098-104). IEEE.

[13] Abubeker, K.M. and Baskar, S., 2023. B2-Net: an artificial intelligence powered machine learning framework for the classification of pneumonia in chest x-ray images. Machine Learning: Science and Technology, 4(1), p.015036.

[14] Chandra, T.B. and Verma, K., 2020. Pneumonia detection on chest x-ray using machine learning paradigm. In Proceedings of 3rd International Conference on Computer Vision and Image Processing: CVIP 2018, Volume 1 (pp. 21-33). Springer Singapore.

[15] Hasoon, J.N., Fadel, A.H., Hameed, R.S., Mostafa, S.A., Khalaf, B.A., Mohammed, M.A. and Nedoma, J., 2021. COVID-19 anomaly detection and classification method based on supervised machine learning of chest X-ray images. Results in Physics, 31, p.105045.

[16] Shaheed, K., Szczuko, P., Abbas, Q., Hussain, A. and Albathan, M., 2023, March. Computer-Aided Diagnosis of COVID-19 from Chest X-ray Images Using Hybrid-Features and Random Forest Classifier. In Healthcare (Vol. 11, No. 6, p. 837). MDPI.

[17] Habib, N. and Rahman, M.M., 2021. Diagnosis of corona diseases from associated genes and X-ray images using machine learning algorithms and deep CNN. Informatics in Medicine Unlocked, 24, p.100621.

[18] Harishvijey, A. and Raja, J.B., 2022. Automated technique for EEG signal processing to detect seizure with optimized Variable Gaussian Filter and Fuzzy RBFELM classifier. Biomedical Signal Processing and Control, 74, p.103450.

[19] Bi, C., Xu, S., Hu, N., Zhang, S., Zhu, Z. and Yu, H., 2023. Identification Method of Corn Leaf Disease Based on Improved Mobilenetv3 Model. Agronomy, 13(2), p.300.

[20] Ahmadi, M., Dashti Ahangar, F., Astaraki, N., Abbasi, M. and Babaei, B., 2021. FWNNet: presentation of a new classifier of brain tumor diagnosis based on fuzzy logic and the wavelet-based neural network using machine-learning methods. Computational Intelligence and Neuroscience, 2021.

[21] Hemeida, M., Osheba, D., Alkhalaf, S., Fawzy, A., Ahmed, M. and Roshdy, M., 2023. Optimized PID controller using Archimedes optimization algorithm for transient stability enhancement. Ain Shams Engineering Journal, 14(10), p.102174.

[22] https://www.kaggle.com/datasets/paultimothymooney/chest-xray-pneumonia

[23] Zhang, D.; Ren, F.; Li, Y.; Na, L.; Ma, Y. Pneumonia Detection from Chest X-ray Images Based on Convolutional Neural Network. Electronics 2021, 10, 1512. https:// doi.org/10.3390/electronics10131512